PROCEEDINGS OF SCIENCE

PoS(CPOD 2009)002

Exploring the QCD phase diagram: Fluctuations and Correlations

Volker Koch*
Lawrence Berkeley National Laboratory
Berkeley, CA 94720, USA
E-mail: vkoch@lbl.gov

In this contribution an attempt is made to provide a status report on the exploration of the QCD phase diagram via the study of fluctuations and correlations in heavy ion collisions.

5th International Workshop on Critical Point and Onset of Deconfinement
June 8-12, 2009
Brookhaven National Laboratory, Long Island, New York, USA

*Speaker.

1. Introduction

The exploration of the QCD phase diagram, both experimentally and theoretically, is one of the main thrusts of present day research in strong interaction physics. Experimentally, hot and dense matter is created in the laboratory via the collision of heavy nuclei, and experiments have been carried out at many facilities, starting from the BEVALAC at moderate center of mass energies of $\sqrt{s} \approx 2.5\,\mathrm{AGeV}$ to RHIC at $\sqrt{s} = 200\,\mathrm{GeV}$ and soon at the Large Hadron Collider (LHC) at $\sqrt{s} \approx 5\,\mathrm{TeV}$. Theoretically, the properties of hot and dense strongly interacting matter are explored with a variety of approaches and strategies, ranging from Lattice QCD to perturbative QCD and effective models. Since interesting structures in the phase diagram such as co-existence regions, critical points etc. are most likely associated with non-perturbative phenomena, at present Lattice QCD (LQCD) is the only available method to explore the phase structure directly within QCD. However, rigorous LQCD calculations so far only allow for the calculation of quantities at vanishing baryon number chemical potential, where it has been shown that the QCD transition, often referred to as the deconfinement or chiral restoration transition, is an analytic cross over [1]. On the other hand, effective chiral models, such as the linear sigma model or the Nambu Jona-Lasinio model, find a first order phase transition at small temperatures and large baryon-number chemical potential (for a review see e.g. [2]). Together with the cross over at zero baryon density, this suggests that there should be a critical endpoint, where the first order coexistence stops. While this is seen in the effective models, so far the existence of a critical end point has not been rigorously established in Lattice QCD. Several methods to explore the region of finite baryon density have been developed [3, 4, 5] but they are restricted to either the region of small baryon-number chemical potential or to systems with small volume. In addition new ideas about a possible "quarkyonic" phase [6] based on large N_c arguments have emerged. As a result, the schematic phase diagram depicted in Fig.1 may indeed be much richer than shown.

While the existence and the location of a QCD critical point, phase co-existence region or other phases is not yet rigorously established theoretically, this should not prevent an experimental exploration of a possible structures in the QCD phase diagram. Indeed, this has been one of the main driving forces of relativistic heavy ion research. By tuning the beam energy one can influence the temperature and density region of the system under investigation. This is evidenced by the systematics of hadronic abundances, see e.g. [7], where the temperature and chemical potential needed to describe the observed hadron abundances change with beam energy. In addition to tuning the beam energy one of course needs robust observables, which indicate that the system has indeed undergone a phase change. This is a rather non-trivial task and we will try to review the status of some of these observables in this contribution.

This contribution is organized as follows: In the next section we briefly remind the reader about the nuclear liquid gas transition. Then we turn to the QCD phase diagram and try to summarize the various techniques that have been developed to explore the existence of a critical point by means of Lattice QCD. After a more general discussion of observables we will then review the present status of some of the observables which already have been measured over a wide range of beam energies.

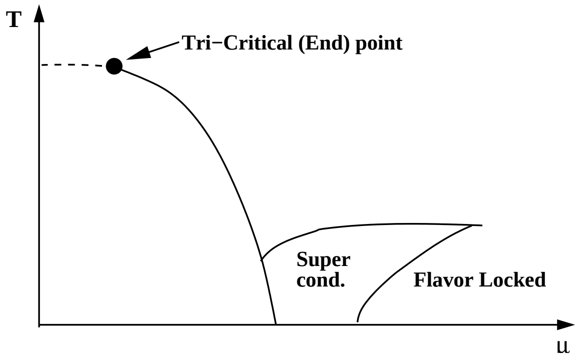

Figure 1: Schematic QCD phasediagram

2. The (Nuclear) Liquid-Gas Phase Transition

Conventional nuclear matter has a first order phase transition from a dense (liquid) to a dilute (gas) phase which ends at a critical point at temperature $T \simeq 16\,\mathrm{MeV}$. The fact that nuclear matter has such a phase transition is not at all surprising. The nuclear force, with its short range repulsion and intermediate range attraction, is very similar to a van der Waals force which is used as a textbook example to introduce real gases with phasetransitions between a gaseous a liquid phase (see e.g.[8]). Therefore, conceptually the phase transition of nuclear matter, often referred to as the "nuclear liquid-gas phasetransition", is rather straightforward and its existence has been predicted already in the seventies, e.g. [9].

In addition, the phases are easily identified even for a small system such as it is produced in a collision of nuclei: the low density (gas) phase is nothing but a gas of nucleons whereas the high density (liquid) phase is made out of droplets or rather clusters of nucleons, often referred to as intermediate mass fragments. This is quite different in case of the QCD transition. There, the low density phase is a hadron gas, which is easily identified but the high density phase is most likely some kind of deconfined matter, which is not so easily detected in an actual experiment.

Experiments searching for the nuclear liquid-gas phasetransition in intermediate energy nuclear collisions have been carried out for more than 20 years and the existence of a liquid-gas co-existence has been established by several different methods (for a recent compilation of the state of the art see [10]). Most relevant for the task of identifying a possible phase co-existence region in the QCD diagram is likely the identification of phenomena related to a spinodal instability [11, 12, 13]. If a system moves sufficiently fast into the co-existence region it can enter the mechanically unstable regime, the spinodal region, which in turn results in dynamical (spinodal) instabilities. These instabilities lead to the formation of blobs of typical size, which is determined by the length scales of the underlying interaction. In case of the nuclear liquid-gas phasetransition, spinodal instabilities were predicted to lead to event classes which are characterized by a very narrow distribution in the size of the final fragments. This has been convincingly observed in experiment by the INDRA collaboration [14].

3. The QCD Phase Diagram

As already mentioned in the introduction, the QCD phase diagram is reasonable well understood for vanishing baryon number. Here, Lattice QCD with staggered fermions finds an analytic crossover [1] at a temperature of $T_c = 170 - 190\,\mathrm{MeV}$. While the actual value of the crossover transition temperature is still being disputed [15, 16], the fact that the transition is a crossover is agreed upon by all Lattice groups. At finite baryon density, or equivalently baryon number chemical potential, μ_B, the situation is less clear. Lattice simulations are very difficult if not impossible to carry out due to the complex phase in the fermion determinant, which arises at finite μ_B. There are, however, several methods to circumvent this problem. On the one hand there are the so-called reweighting methods. The pioneering work [17] in this approach has indeed located a critical point. With realistic quark masses, this method predicts its location at $T \simeq 160 MeV$ and $\mu_B \simeq 360\,\mathrm{MeV}$ [3]. However, the method employed can not easily be extended to larger volumes and, therefore, one does not know if the signal survives in the infinite volume limit. Other approaches calculate the free energy at finite chemical potential as a Taylor expansion in terms of the chemical potential (see e.g [5, 18]). The expansion coefficients are given by the baryon number cumulants or susceptibilities. While this method does not allow to extract a critical point directly it can provide limits for its location. At present a conservative limit for its chemical potential is $\mu_B \gtrsim T_c$ ([5, 19]), where $T_c \sim 180\,\mathrm{MeV}$ is the transition temperature at vanishing baryon number density.

Another way to analyze models and also Lattice QCD results in the region of small chemical potentials is to find the critical quark mass for which one obtains a second order transition [20]. This is depicted in Fig.2. Most chiral models predict that the critical quark mass increases with the chemical potential (right panel of Fig.2). In this case, one expects a critical point at finite chemical potential once the critical quark mass coincides with the physical quark mass, as can be seen in the figure. Lattice QCD, on the other hand, seems to favor the opposite trend, namely a decreasing critical quark mass (left panel of Fig.2). This is the result of [20, 21] obtained in an expansion up to fourth order in the chemical potential μ_B on a rather small lattice. If these lattice results hold up for larger lattices it seems that the chiral dynamics does not predict the small μ_B behavior of the critical quark mass correctly and other effects are more dominant. One possibility would be a repulsive vector coupling, which is neither constrained nor ruled out by symmetry arguments. As shown in [22] a suitable choice of a repulsive vector coupling can indeed reproduce the trend seen on the lattice. However, at this conference O. Phillipsen reported first results with larger lattices where he sees a somewhat reduced curvature, consistent with zero. Therefore, at present, the situation is still open. Also, calculations in a linear sigma model including thermal fluctuations finds two critical points [23] for a pion mass of $m_\pi = 35\,\mathrm{MeV}$, indicating that the critical surface depicted in Fig.2 may bend back at higher temperatures. For a physical pion mass, this model exhibits only one critical point at large μ_B consistent with all other mean field treatments of the sigma and Nambu Jona-Lasinio model (for a compilation see [2]).

Obviously there is only limited theoretical guidance for an experimental search for the critical point as the model predictions for its location vary quite a bit. From hadronic freeze out systematics [7], on the other hand, one knows that the chemical potential of the system created depends on the center-of-mass energy of the collision. Unless the temperature of the critical point is unexpectedly low, one can explore regions up to about $\mu_B \leq 500\,\mathrm{MeV}$ in the chemical potential by lowering the

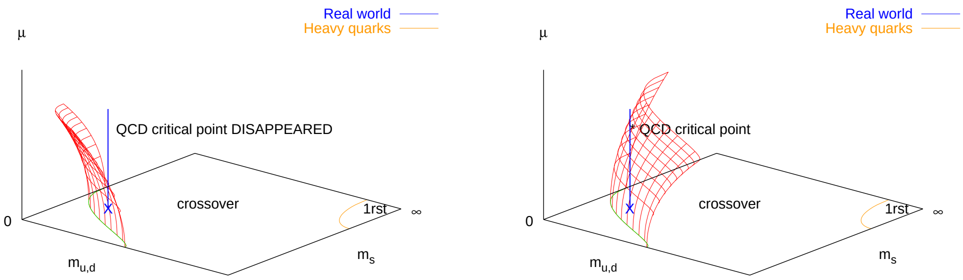

Figure 2: Behavior of the critical line as a function of chemical potential μ_B. Left panel: Scenario favored by Lattice QCD [20, 21] where critical line moves towards smaller quark masses. Right panel: Standard scenario predicted by most chiral models, where critical line moves towards higher quark masses. The figure is adapted from [20].

beam energy to about $\sqrt{s} \simeq 5\,\mathrm{GeV}$. Hence, the strategy for a search is to study excitation functions of various observables and see if they show non-monotonic behavior at the same beam energy, indicating the location of the critical point or of the first order phase co-existence region

4. Fluctuation and Correlations: From theory to observables

Fluctuations and correlations are unique signatures for phase transitions. Therefore, an experimental search for a possible critical point and a first order co-existence region in the QCD phase diagram is intimately connected with the study and measurement of fluctuations and correlations. Before we will discuss presently available data let us briefly review the underlying concepts of fluctuations and correlation in the context of the system in thermodynamic equilibrium.

A system in thermal equilibrium (for a grand-canonical ensemble) is characterized by its partition function

$$Z = \mathrm{Tr}\left[\exp\left(-\frac{H - \sum_i \mu_i Q_i}{T}\right)\right] \tag{4.1}$$

where H is the Hamiltonian of the system, and Q_i and μ_i denote the conserved charges and the corresponding chemical potentials, respectively. In case of three flavor QCD these are strangeness, baryon-number, and electric charge, or, equivalently, the three quark flavors up, down, and strange. The mean and the (co)-variances are then expressed in terms of derivatives of the partition function with respect to the appropriate chemical potentials,

$$\langle Q_i \rangle = T \frac{\partial}{\partial \mu_i} \log(Z) \tag{4.2}$$

$$\langle \delta Q_i \delta Q_j \rangle = T^2 \frac{\partial^2}{\partial \mu_i \partial \mu_j} \log(Z) \equiv V T \chi_{i,j} \tag{4.3}$$

with $\delta Q_i = Q_i - \langle Q_i \rangle$. Here we have introduced the susceptibilities

$$\chi_{i,j} = \frac{T}{V} \frac{\partial^2}{\partial \mu_i \partial \mu_j} \log(Z) \tag{4.4}$$

which are generally quoted as a measure of the (co)-variances. The diagonal susceptibilities, $\chi_{i,i}$, are a measure for the fluctuations of the system, whereas the off-diagonal susceptibilities, $\chi_{i,j}$; $i \neq j$, characterize the correlations between the conserved charges Q_i and Q_j. We note that the susceptibilities are directly related to the well known cumulants in statistics [24].

One can define and study higher order susceptibilities or cumulants, by differentiating multiple times with respect to the appropriate chemical potentials

$$\chi^{(n_i,n_j,n_k)} \equiv \frac{1}{VT} \frac{\partial^{n_i}}{\partial(\mu_i/T)^{n_i}} \frac{\partial^{n_j}}{\partial(\mu_j/T)^{n_j}} \frac{\partial^{n_k}}{\partial(\mu_k/T)^{n_k}} \log Z. \tag{4.5}$$

Higher order cumulants up to the sixth [18, 25, 26, 27] and even eighth [5] order have been calculated in Lattice QCD.

Susceptibilities are related to integrals of equal time correlation functions of the appropriate charge-densities. Here we will restrict ourselves to the second order susceptibilities keeping in mind that the higher order susceptibilities can also be expressed in terms of appropriate (higher order) correlation functions.

Consider a density fluctuation $\delta\rho_i(x) = \rho_i(x) - \bar{\rho_i}$ at location x, where $\bar{\rho_i}$ denotes the spatially averaged density of the charge Q_i. Then the susceptibilities are given by the following integral over the density-density correlation functions:

$$\chi_{i,j} = \frac{1}{VT} \int d^3x d^3y \left\langle \delta\rho_i(x)\, \delta\rho_j(y) \right\rangle = \frac{1}{T}\bar{\rho_i}\delta_{i,j} + \frac{1}{T}\int d^3r C_{i,j}(r). \tag{4.6}$$

The correlation functions

$$C_{i,j}(\vec{r}) = \left\langle \delta\rho_i(\vec{r})\, \delta\rho_j(0) \right\rangle - \bar{\rho_i}\delta_{i,j}\delta(\vec{r}) \sim \frac{\exp\left[-r/\xi_{i,j}\right]}{r} \tag{4.7}$$

are characterized by typical correlation lengths $\xi_{i,j}$. The correlation length provides a measure for the strength and type of the correlation. For example, in case of a second order phase transition the correlation length diverges with a characteristic critical exponent, usually denoted as ν.

To illustrate this point let us first consider the case of a classical ideal gas. This will also serve as useful reference for comparison with LQCD results. Since a classical ideal gas has no correlations, by construction its correlation functions vanish, $C_{\text{ideal gas}} = 0$, and the susceptibilities are given by the first, local term in Eq. 4.6, $\sim \bar{\rho_i}\delta_{i,j}$, implying that all co-variances vanish. As a consequence, the fluctuations are proportional to the number of particles in the system, and thus grow linearly with the system size, V.

$$\left\langle (\delta Q_i)^2 \right\rangle \sim V \tag{4.8}$$

The more relevant case concerning the QCD critical point corresponds to a second order phase transition. In this case, the correlation length diverges at the critical temperature

$$\xi \sim |T - T_c|^{-\nu} \tag{4.9}$$

where $\nu > 0$ is relevant critical exponents characterizing a second order phase transition in a given universality class [28]. In this case, the volume dependence of the susceptibilities is governed by the integral of the correlation function

$$\chi_{i,j} \sim \xi^2 \sim V^{2/3} \tag{4.10}$$

so that the fluctuations grow like[1]

$$\left\langle (\delta Q_i)^2 \right\rangle \sim V^{5/3}, \ \text{second order}. \tag{4.11}$$

In case of a first order transition we have co-existence of phases with different densities, and the correlation function is a constant, $C(r) = const \neq 0$. Consequently, the fluctuations scale like

$$\left\langle (\delta Q_i)^2 \right\rangle \sim V^2, \ \text{first order}. \tag{4.12}$$

Most other systems, including systems with a cross over, such as QCD at vanishing chemical potential [1], will exhibit a finite correlation length. Consequently, the susceptibility is independent of the volume, and the fluctuations scale linearly with the volume, just as in the case of an ideal gas

$$\left\langle (\delta Q_i)^2 \right\rangle \sim V, \ \text{no phase} - \text{transition}. \tag{4.13}$$

In principle, one could utilize the above volume scaling of the fluctuations in heavy-ion experiments by studying the system size dependence of, e.g., baryon-number fluctuations. However, in case of the second order phase-transition, the phenomenon of critical slowing down limits the actual size of correlation length due to the finite life-time of the system created in these collisions. A maximum correlation length of $\xi \sim 2.5\,\text{fm}$ has been estimated in ref. [29] which is much smaller than the typical size of a system created in these reactions. Consequently, such a system would just behave like any other with a constant correlation-length and, therefore, would not exhibit the system size dependence discussed above.

After these more formal consideration let us next turn to actual observables. Since the baryon density is an order parameter for the phase transition at finite density, baryon number fluctuations are the natural observable to consider. However, as discussed in detail in [30] baryon number conservation imposes serious limitations on this observable, especially for low center-of-mass energies. In addition, the measurement of the baryon number requires the detection of neutrons, which is difficult. As argued in [31], it may be sufficient to study proton number fluctuations, as the iso-vector channel does not show critical behavior. However, if the baryon-number fluctuations are suppressed due to global baryon-number conservation, one has to be careful that the remaining fluctuations, which one observes in an actual experiment, are not simply isospin fluctuations. Those will not be indicative of the QCD phase structure at finite density.

In addition, even if the system reaches the critical point, the correlation length, which diverges in a thermal system, would be finite due to critical slowing down together with the finite time the system has to develop the correlations. In [29] a correlation length of $\xi \simeq 2.5\,\text{fm}$ has been estimated based on these considerations. Therefore, it may be advantageous to study higher order cumulants which depend on higher powers of the correlations length [32]. Indeed the fourth order cumulant $\chi^{(4)}$ scales like the seventh power of the correlation length, $\sim \xi^7$ [32]. Thus if the correlation length increases only by 10% in the vicinity of the critical point, one should see an enhancement by a factor of two in the fourth order cumulant, whereas the second order cumulant, i.e. the fluctuations, would only increase by 20%. A first measurement of these higher order cumulants has been carried

[1] The correct scaling of the susceptibility with the volume actually involves the critical exponents, $\chi \sim V^{\gamma/(3\nu)}$. Our example here is correct for so called mean field exponents. For details see [28].

out by the STAR collaboration at full RHIC energies [33], where no significant signal is found, consistent with expectations based on the absence of any phase transition at small μ_B.

Initially transverse momentum fluctuations have been proposed as a signature for the critical point [34, 35], since close to the critical point the system should develop large, and mostly long range, i.e low momentum, fluctuations. Therefore, it was suggested that an excitation function of the transverse momentum fluctuations should show non-monotonic behavior, especially for small transverse momenta. In the meantime, such an excitation function has been measured and it is shown in Fig.3 for different charge combinations and different cuts on the transverse momentum. Critical fluctuations, corrected for critical slowing down and expansion of the system [29] would lead to a bump which should be at least a factor of two larger than the statistical background. Obviously, the data shown in Fig.3 do not show such a behavior, even for small transverse momenta. The results at RHIC [36] are consistent with the data from SPS. Hence, so far there is no indication of a critical point in the transverse momentum fluctuation measurements. Of course it could be that the signal is too weak to be seen and it may also be washed out by subsequent hadronic interactions. To address this issue, higher cumulants, as discussed above, need to be measured as they should show a stronger enhancement close to the critical point. Furthermore, on the theoretical side, one needs to get a better understanding of the degradation of the proposed signals in the hadronic phase.

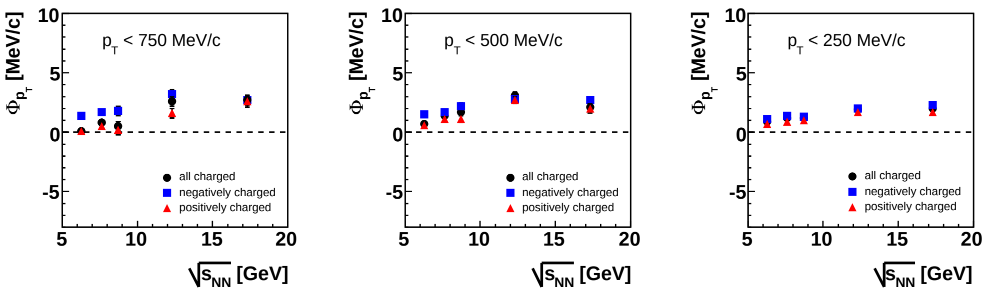

Figure 3: Preliminary data on the energy dependence of p_t fluctuations from the NA49 collaboration [37] for all charged particles and for positively and negatively charged particles. The panels show the fluctuations for different cuts in the transverse momentum. The figure is adapted from [37].

The only observable which shows a strong beam energy dependence are the fluctuations of the kaon-to-pion ratio, shown in Fig.4, and neither a transport approach nor the statistical hadron gas model can reproduce these data [38, 39]. However, $\sigma^2_{\rm dynamic}$ scales with the inverse *accepted* multiplicity (see e.g. [30]), and the observed rise may very well be partially due to the changing acceptance of the fixed target NA49 experiment. That this may actually be the case, has been investigated in [40], where several scaling prescriptions have been used to predict the excitation function of the kaon to pion ratio fluctuations. The results, shown in Fig.4, indicate that a large part of this enhancement may actually be due to the dependence of $\sigma_{dynamical}$ on the multiplicity of accepted particles. While an additional enhancement cannot be ruled out at this time, it is still not clear if it would be related to the critical point. Close to the critical point one would expect the fluctuations of the pion number to be enhanced. But this would imply also enhanced fluctuations

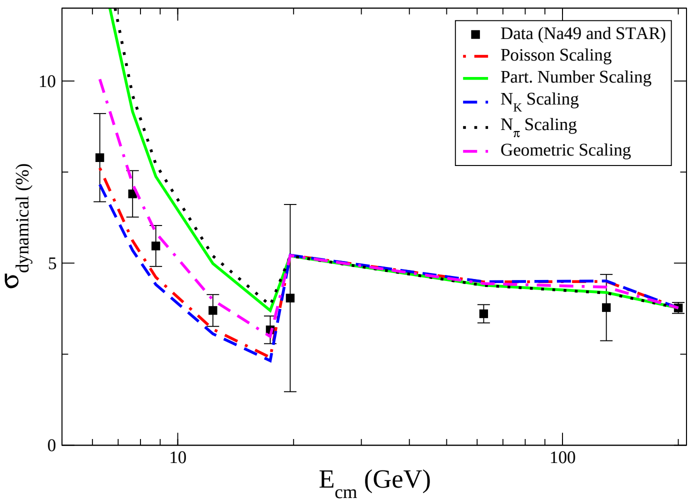

Figure 4: Fluctuations of the kaon to pion ratio as a function of beam energy. The data are from the NA49 [38] and the STAR collaboration [41]. The lines represent several ways to scale the $\sqrt{s} = 200\,\mathrm{GeV}$ data taking into account the actual accepted multiplicities. For details see [40].

of the proton-to-pion ratio, which is not observed in experiment [38], where the data are well reproduced by the URQMD calculations. In addition, in this case the effects due to multiplicity scaling are small [40].

While most of the attention is presently on the QCD critical point and its detection, let us emphasize that it might be more beneficial to look for and identify the first order co-existence region. Finding one implies finding the other as they are intimately related. Contrary to the critical *point*, the first order transition corresponds to an entire *region* in the $T-\rho$ phase diagram. Thus it is more likely for the system to cross this region rather than the critical point. It is also more likely for the system to spend sufficient time in this region in order to develop measurable effects. One example is the development of spinodal instabilities, which are a generic phenomenon of dynamical first order transitions [11]. Spinodal instabilities have been studied and successfully identified in the context of the nuclear liquid gas phase transition [14]. In the case of the QCD first order transition, spinodal instabilities could lead to kinematic correlations among particles [13] and to enhanced fluctuations of strangeness [42]. And indeed the observed enhancement of the kaon-to-pion fluctuations, if real, may be due to these enhanced fluctuations in the strangeness sector [42]. However, just as for the critical point, there has been no quantitative calculation of the effect due to hadronic re-scattering on the observables. In addition, presently there is no dynamical model which carries the system through the spinodal region. In the case of the nuclear liquid gas phase-transition such models proved to be extremely useful in guiding the experimental searches. These models have also helped to develop unique observables, such as the variance of the cluster size which subsequently could be identified in experiment[14]. This analysis lead to a rather convicing case for the existence of a first order phase co-existence region for nuclear matter. In order to build a similar dynamical model for the QCD case, additional information is needed. While fluid-dynamics appears to be a reasonable framework, it needs to be extended to include finite range effects. It is these finite range effects which determine the typical size of the blobs created by the dynamical instability characteristic of the spinodal region. A first step towards such a development has been carried out in [43] and has been reported at this conference. But the development of [43] requires the knowledge of a length scale characterizing the finite range effects. At present this is not known for the QCD phasetransition whereas in case of the nuclear liquid gas transition it is directly associated with the range of the nuclear interaction. One way to extract this information is to study the interface energy and thickness in lattice QCD.

Although this contribution is about fluctuations, in closing let us briefly mention other observables which are discussed in the context of the critical point. Most prominently is the idea to look for soft modes in the low-mass dilepton invariant mass spectrum. However, it is not clear if the soft modes, responsible for the large density fluctuations close to the critical point, are visible in the dilepton channel, since they are of space-like origin. Indeed, an analysis of the fluctuations close to the critical point carried out in the Nambu model with finite quark masses [44, 45] shows that the sigma-meson remains gaped at the critical point, contrary to the chiral transition in the limit of vanishing quark masses. Thus, in this model no significant change due to the critical point has been seen in the time-like spectrum, which is accessible to dilepton spectroscopy.

There are a number of other possibilities which have not yet been explored theoretically. For example, it maybe interesting to further explore the co-variances between the baryon density fluctuations and other quantities which couple to the baryon density, such as e.g. dileptons. These co-variances are expected to become large and could possibly be developed into practical observables, which will not be affected by baryon number conservation.

5. Conclusions

To conclude, let us remind ourselves that the field of relativistic heavy ion collisions started out with the quest to find and identify the QCD phase transition. While many interesting phenomena have been discovered on the way, such as the surprisingly large elliptic flow, the quest is still on. In view of the fact that Lattice QCD predicts the transition at vanishing baryon density to be a crossover, going to even higher energies is not the right direction to explore structures in the QCD phasediagram. Instead, a beam energy scan towards lower energies, as planned for RHIC, is the right way to explore the phasediagram in the high density region, where true phase transition are expected. For such a program to be successful one needs not only guidance from theory for the location of a possible phase transition but also for observables that are most sensitive and robust for an actual measurement. This aspect is not yet very well developed, and it may be useful to adapt some of the strategies developed for the identification of the nuclear liquid gas phase transition.

Acknowledgments

This work is supported by the Director, Office of Energy Research, Office of High Energy and Nuclear Physics, Divisions of Nuclear Physics, of the U.S. Department of Energy under Contract No. DE-AC02-05CH11231.

References

[1] Y. Aoki, G. Endrodi, Z. Fodor, S. D. Katz, and K. K. Szabo *Nature* **443** 675–678 (2006) , `arXiv:hep-lat/0611014`.

[2] M. A. Stephanov *Prog. Theor. Phys. Suppl.* **153** 139–156 (2004) , `arXiv:hep-ph/0402115`.

[3] Z. Fodor and S. D. Katz *JHEP* **04** 050 (2004) , `arXiv:hep-lat/0402006`.

[4] M. Cheng *et al. Phys. Rev.* **D79** 074505 (2009) , `arXiv:0811.1006 [hep-lat]`.

[5] R. V. Gavai and S. Gupta `arXiv:0806.2233 [hep-lat]`.

[6] L. McLerran and R. D. Pisarski *Nucl. Phys.* **A796** 83–100 (2007) , `arXiv:0706.2191 [hep-ph]`.

[7] P. Braun-Munzinger, K. Redlich, and J. Stachel `nucl-th/0304013`.

[8] F. Reif, *Fundamentals of Statistical and Thermal Physics*. McGraw-Hill, 1984.

[9] G. Sauer *Nucl. Phys.* **A264** 221 (1976) .

[10] "Dynamics and thermodynamics with nuclear degrees of freedom." Eur. phys. j a31, 2006.

[11] P. Chomaz, M. Colonna, and J. Randrup *Phys. Rept.* **389** 263–440 (2004) .

[12] J. Randrup *Phys. Rev. Lett.* **92** 122301 (2004) , `arXiv:hep-ph/0308271`.

[13] J. Randrup *Acta Phys. Hung.* **A22** 69–82 (2005) .

[14] B. Borderie *et al.*, **INDRA** Collaboration *Phys. Rev. Lett.* **86** 3252–3255 (2001) , `arXiv:nucl-ex/0103009`.

[15] M. Cheng *et al. Phys. Rev.* **D74** 054507 (2006) , `arXiv:hep-lat/0608013`.

[16] Y. Aoki, Z. Fodor, S. D. Katz, and K. K. Szabo *Phys. Lett.* **B643** 46–54 (2006) , `arXiv:hep-lat/0609068`.

[17] Z. Fodor and S. D. Katz *JHEP* **03** 014 (2002) , `hep-lat/0106002`.

[18] C. R. Allton *et al. Phys. Rev.* **D71** 054508 (2005) , `hep-lat/0501030`.

[19] F. Karsch, **RBC** Collaboration `arXiv:0804.4148 [hep-lat]`.

[20] P. de Forcrand and O. Philipsen *JHEP* **01** 077 (2007) , `arXiv:hep-lat/0607017`.

[21] P. de Forcrand and O. Philipsen `arXiv:0808.1096 [hep-lat]`.

[22] K. Fukushima `arXiv:0809.3080`.

[23] E. S. Bowman and J. I. Kapusta *Phys. Rev.* **C79** 015202 (2009) , `arXiv:0810.0042 [nucl-th]`.

[24] M. Abramowitz and I. A. Stegun, *Handbook of Mathematical Functions*. Dover Publications, 1972.

[25] R. V. Gavai and S. Gupta *Phys. Rev.* **D73** 014004 (2006) , `hep-lat/0510044`.

[26] C. Schmidt, **RBC-Bielefeld** Collaboration `arXiv:0805.0236 [hep-lat]`.

[27] C. Schmidt, **RBC-Bielefeld** Collaboration `arXiv:0810.0375 [hep-lat]`.

[28] L. Landau and L. Lifshitz, *Statistical Physics*. Pergamon Press, New York, 1980.

[29] B. Berdnikov and K. Rajagopal *Phys. Rev.* **D61** 105017 (2000) , `hep-ph/9912274`.

[30] V. Koch arXiv:0810.2520 [nucl-th].

[31] Y. Hatta and M. A. Stephanov *Phys. Rev. Lett.* **91** 102003 (2003) , arXiv:hep-ph/0302002.

[32] M. Stephanov arXiv:0809.3450[hep-ph].

[33] T. K. Nayak and for the STAR Collaboration arXiv:0907.4542 [nucl-ex].

[34] M. A. Stephanov, K. Rajagopal, and E. V. Shuryak *Phys. Rev. Lett.* **81** 4816–4819 (1998) , hep-ph/9806219.

[35] M. A. Stephanov, K. Rajagopal, and E. V. Shuryak *Phys. Rev.* **D60** 114028 (1999) , hep-ph/9903292.

[36] J. Adams *et al.*, **STAR** Collaboration *Phys. Rev.* **C71** 064906 (2005) , arXiv:nucl-ex/0308033.

[37] K. Grebieszkow *et al.*, **NA49** Collaboration *PoS* **CPOD07** 022 (2007) , arXiv:0707.4608 [nucl-ex].

[38] C. Alt *et al.*, **NA49** Collaboration arXiv:0808.1237 [nucl-ex].

[39] G. Torrieri *Int. J. Mod. Phys.* **E16** 1783–1789 (2007) , arXiv:nucl-th/0702062.

[40] V. Schuster *in preparation* .

[41] B. Abelev *et al.*, **STAR** Collaboration arXiv:0901.1795 [nucl-ex].

[42] V. Koch, A. Majumder, and J. Randrup *Phys. Rev.* **C72** 064903 (2005) , arXiv:nucl-th/0509030.

[43] J. Randrup *Phys. Rev.* **C79** 054911 (2009) , arXiv:0903.4736 [nucl-th].

[44] H. Fujii and M. Ohtani arXiv:hep-ph/0403039.

[45] H. Fujii and M. Ohtani *Prog. Theor. Phys. Suppl.* **153** 157–164 (2004) , arXiv:hep-ph/0401028.